Antagonistic factors control the unproductive splicing of SC35 terminal intron

Natacha Dreumont, Sara Hardy, Isabelle Behm-Ansmant, Liliane Kister, Christiane Branlant, James Stevenin, Cyril Bourgeois

Published online 3 December 2009

Nucleic Acids Research, 2010, Vol. 38, No. 4 ***1353–1366***
doi:10.1093/nar/gkp1086

Antagonistic factors control the unproductive splicing of *SC35* terminal intron

Natacha Dreumont[1,2,3,4], Sara Hardy[1,2,3,4], Isabelle Behm-Ansmant[5], Liliane Kister[1,2,3,4], Christiane Branlant[5], James Stévenin[1,2,3,4,*] and Cyril F. Bourgeois[1,2,3,4,*]

[1]IGBMC Department of Functional Genomics, [2]INSERM U964, [3]CNRS UMR 7104, 67400 Illkirch, [4]University of Strasbourg, 67000 Strasbourg and [5]UMR CNRS-UHP 7214 AREMS, Université Henri Poincaré, 54506 Vandoeuvre-les-Nancy, France

Received June 26, 2009; Revised and Accepted November 6, 2009

ABSTRACT

Alternative splicing is regulated in part by variations in the relative concentrations of a variety of factors, including serine/arginine-rich (SR) proteins. The SR protein SC35 self-regulates its expression by stimulating unproductive splicing events in the 3′ untranslated region of its own pre-mRNA. Using various minigene constructs containing the terminal retained intron and flanking exons, we identified in the highly conserved last exon a number of exonic splicing enhancer elements responding specifically to SC35, and showed an inverse correlation between affinity of SC35 and enhancer strength. The enhancer region, which is included in a long stem loop, also contains repressor elements, and is recognized by other RNA-binding proteins, notably hnRNP H protein and TAR DNA binding protein (TDP-43). Finally, *in vitro* and *in cellulo* experiments indicated that hnRNP H and TDP-43 antagonize the binding of SC35 to the terminal exon and specifically repress the use of *SC35* terminal 3′ splice site. Our study provides new information about the molecular mechanisms of SC35-mediated splicing activation. It also highlights the existence of a complex network of self- and cross-regulatory mechanisms between splicing regulators, which controls their homeostasis and offers many ways of modulating their concentration in response to the cellular environment.

INTRODUCTION

Alternative splicing (AS) occurs during the expression of most genes and has important functions in many biological processes. Some of the mechanisms controlling the alternative choice of splice sites made by cells in response to various intra or extracellular stimuli are now better understood, yet many molecular aspects of splicing regulation remain unclear. One key feature of AS regulation is the existence of a 'splicing code' based on the antagonistic assembly of activator and repressor complexes onto a variety of *cis*-acting enhancer and silencer elements, allowing the activation or repression of alternative splice sites (1). This relies largely on the relative concentrations of available splicing activators and repressors. Two major families of proteins mediate the interactions between *cis*-regulatory elements and the spliceosomal machinery: serine/arginine-rich (SR) proteins (2,3) and hnRNP proteins (4). AS is also influenced by its dynamic coupling to transcription and other mRNA processing events (5), or by the formation of RNA secondary structures (6).

A well-known function of AS is to expand the diversity of the proteome, however a large proportion (about one third) of AS events create premature stop codons that are predicted to elicit the nonsense-mediated mRNA decay (NMD) pathway and to result in the specific degradation of those mRNAs. Although recent studies do not support a widespread impact of this phenomenon (called AS-NMD) on gene expression, it clearly influences the expression of some genes by inducing variations in the production of specific mRNA isoforms (7). A few years ago, we and our collaborators described a negative feedback loop controlling the expression of the SR

*To whom correspondence should be addressed. Tel: +33 38 86 53 361; Fax: +33 38 86 53 201; Email: stevenin@igbmc.fr
Correspondence may also be addressed to Cyril F. Bourgeois. Institute of Molecular Biology and Pathology of CNR, Department of Genetics and Molecular Biology, University of Rome 'Sapienza', P.le Aldo Moro 5, 00185 Rome, Italy. Tel: +39 64 99 12 217; Fax: +39 64 99 12 500; Email: cyril.bourgeois@inserm.fr
Present address:
Sara Hardy, Institut de Recherches Cliniques de Montréal, Montréal H2W 1R7, Canada.

protein SC35 through AS-NMD (8). The SC35-encoding gene is essential and conditional knockout experiments in mouse or in embryonic fibroblasts have shown that SC35 is involved in the maintenance of genomic stability and in the control of cell proliferation in thymus and pituitary gland (9,10). These important biological functions presuppose a finely tuned control of SC35 expression in the cell. Indeed, high SC35 concentration activates distinct splicing events within the 3′ untranslated region (3′ UTR) of its own pre-mRNA, resulting in the formation of mRNA isoforms in which the natural stop codon is located far upstream from the following exon–exon junction (8). The NMD machinery considers this stop codon as premature and triggers the degradation of the corresponding mRNAs (8,11–13).

Other feedback regulation loops have been described for mammalian SR proteins SRp20, 9G8 and Tra2β1 (14–16), and similar cross-regulatory mechanisms exist between the highly related TIA1 and TIAR proteins (17) and between PTB and its paralogs nPTB and ROD1 (18,19). One consequence of those AS events can be the production of truncated protein isoforms. However, a series of bioinformatics and biological studies have recently shown that regulation by evolutionary conserved AS-NMD is a mode of regulation of gene expression common to the entire SR family, several hnRNP proteins and core spliceosomal components (12,20–22). These findings suggest the existence of an integrated network of homeostatic control of the expression of splicing factors, based on complex AS regulatory mechanisms, which are still largely unknown. However, sequence elements that are ultraconserved (elements longer than 200 bp with 100% identity in human, rat and mouse genes) or highly conserved (identity over >100 bp) were suggested to participate to those mechanisms (12,21,23).

Here, we studied the molecular mechanisms of SC35-dependent AS within the 3′ UTR of the *SC35* pre-mRNA. This model is particularly interesting since only a few examples of SC35-mediated regulation of splicing have been studied in detail. We found that splicing of the terminal intron is activated via multiple low-affinity SC35-binding sites located within a highly conserved stem-loop region of the downstream exon. The same regulatory sequence is also bound by several proteins, including hnRNP H and TDP-43, which compete with SC35 binding and antagonize its effect to repress terminal intron splicing *in vitro* and *in cellulo*. Our results improve our knowledge on the splicing activator function of SC35 and reveal complex cross-regulatory mechanisms for the expression of splicing regulators.

MATERIALS AND METHODS

Plasmids

The previously described *SC35*-RI plasmid (wt-RI) (8) was modified by point mutations to create unique restriction sites within exon 2, in positions +3 (*Nhe*I), +38 (*Afl*II) and +74 (*Bam*HI) relative to the 3′ splice site. The resulting pre-mRNA was spliced *in vitro* as the original *SC35*-RI.

To create the p*SC35*-βGlo plasmid, we inserted an *Mfe*I–*Mfe*I PCR fragment (corresponding to the last 237 nt of *SC35* terminal intron followed by 172 exonic nts) into a unique *Mfe*I site located in the middle of rabbit β-globin intron 2 from the pXJ41 plasmid (24).

The sequence used for enzymatic probing, including four intronic nts and the first 106 nts of *SC35* terminal exon, was cloned into *Eco*RI and *Bam*HI of the pGEM-3zf(+) plasmid (Promega). Other constructs are described in the Supplementary Data.

Proteins

Purification of full-length recombinant SC35, ASF/SF2, hnRNP A1 and of GST-SC35ΔRS and GST-9G8ΔRS is described by Cavaloc *et al*. and Gallego *et al*. (25,26). Detailed purification of His6-hnRNP H RRM1-2, GST-hnRNP H and GST-TDP-43 is described in Supplementary Data.

Antibodies

Antibodies raised against a carboxyl-terminal peptide of SC35 (1SC-4F11) and an amino-terminal peptide of ASF/SF2 (1D7) were used previously (25). The antibodies anti-PSF/SFPQ (B92) and anti-PTB/hnRNP I (SH54) were procured from Abcam and Calbiochem, respectively. Other antibodies were kindly provided by D. Auboeuf (anti-p68/DDX5), D. Elliott (anti-SAFB2), D. Black (anti-hnRNP H), S. Rousseau (anti-DAZAP1), E. Buratti (anti-TDP-43) and G. Dreyfuss (anti-hnRNP A1).

RNA affinity chromatography

RNA affinity experiments and MALDI-TOF mass spectrometry analysis were carried out essentially as described by Venables *et al*. (24), with minor modifications which are detailed in the Supplementary Data. Several independent experiments were performed. Proteins for which the peptide coverage score was significantly and reproducibly higher with RNA I and/or RNA II than with control RNA in at least two experiments were considered as 'specific'. Specific binding of some of those proteins was confirmed by western-blotting.

RNA secondary structure analysis by RNase footprinting

In vitro transcribed 5′-end labeled RNA (25 fmol) was pre-incubated in buffer D for 10 min at 65°C, in the presence of 2 μg tRNA, followed by a slow cooling. The renatured RNA was then incubated for 30 min at 20°C in the absence or in the presence of recombinant SC35 (8, 16 and 32 pmol) or hnRNP H RRM1-2 (10, 30 and 50 pmol) in 10 μl of buffer D. Digestion was carried out for 6 min at 20°C in the presence of 0.0005 U of the double-stranded specific RNase V1 (Kemotex), 1 U of RNase T1 (Roche) or 1 U of RNase T2 (Invitrogen), that cleave respectively after G residues or any nucleotide (but preferentially after A residues). In the conditions used, both enzymes preferentially cleave single strands. The production of a

single nucleotide or of a G residue ladder and the arrest of the reactions were carried out as described by Jacquenet *et al.* (27). The cleavage products were fractionated by electrophoresis on a 10% polyacrylamide-8 M urea gel. The free energie of the 2D structure of the SC35 RNA was calculated at 37°C and in 1M NaCl with the Mfold software (28).

RNA-protein UV cross-linking

UV cross-linking assays were carried out in splicing conditions as described by Venables *et al.* (24), using a fixed amount of various RNA probes and different combinations of purified recombinant proteins, as detailed in the figure legend, and in the presence of 0.1 µg *Escherichia coli* tRNA. After cross-linking and digestion with RNases A and T1, complexes were analysed by SDS-PAGE and autoradiography.

In vitro splicing

In vitro splicing assays were performed and quantified as described by Disset *et al.* (29). When transcripts with different backbones (*SC35*-RI and Sp1-derived transcripts) were used in the same experiment and compared one to another (Figure 6 and Supplementary Figure S5), we incubated the samples in various conditions of temperature (between 26 and 30°C) and time (1.5–2 h) in order to obtain equivalent basal splicing efficiency.

Transfections and RT–PCR analysis

HeLa cells were transfected in 6-well plates, at 50% confluency (30% for siRNA experiments), using lipofectamine 2000 (Invitrogen) according to the manufacturer's instructions. The following amounts of transfected plasmids were used: 200 ng of p*SC35*-βGlo reporter, 20 ng of pGFP-SC35 (a gift from J. Soret) and 500 ng of pXJ41-hnRNP H or pTT3-FLAG-TDP-43. In all transfections, 2 µg of total DNA was added per well. To prevent promoter squelching effects, the total amount of CMV promoter-containing plasmid was adjusted to 1 µg with pGL4-CMV plasmid, derived from pGL4 (Promega). For caffeine treatment, cells were first transfected for 24 h with the p*SC35*-βGlo minigene and then treated for 24 h with 14 mM caffeine before RNA and protein extraction. For siRNA treatment, two successive applications of 100 nM siRNAs (Eurogentec) were carried out at 24 h interval. Cells were transfected 24 h after the second siRNA treatment with the reporter plasmid and harvested the next day. Sequences of siRNA were as follows: TDP-43: 5′-GAUGAGAACGAUGAGCCCA-3′ or 5′-AGGCUCAUCUUGGCUUUGC-3′; hnRNP H1/F: 5′-GUUCUUCUCAGGGUUGGAA-3′ or 5′-GGAAGAAAUUGUGCAGUUC-3′; Renilla luciferase: 5′-GUAGCGCGGUGUAUUAUAC-3′. RNAs were extracted using TRI Reagent (Sigma-Aldrich), DNAse I-treated (Roche) and analysed by RT–PCR with the following primers: forward, 5′-ACGGTGCATTGGAACGGACC-3′ and reverse, 5′-TAACCATTATAAGCTGCAAT-3′. The intensity of the bands corresponding to the two mRNAs was quantified using a Typhoon 8600 Imager and the ImageQuant software (GE Healthcare Life Sciences) and corrected to take the relative product size into account. The ratio inclusion/skipping from three independent transfection experiments was normalized using the control sample of each series as a reference, which gave a score for inclusion or skipping of the alternative exon. Proteins were extracted in a buffer containing 50 mM Tris–HCl pH 6.8, 20 mM EDTA, 5% SDS, sonicated briefly and analysed by SDS–PAGE and western blotting.

RESULTS

Splicing of terminal *SC35* intron requires specific downstream exonic sequences

We showed previously that SC35 promotes the inclusion of an alternative cassette exon and the excision of the terminal retained intron in the 3′ UTR of its own transcripts (8). We analysed the molecular mechanisms involved in the excision or retention of terminal *SC35* intron, first using an *in vitro* system which recapitulates its SC35-dependent splicing (Figure 1A). As shown by Sureau *et al.* (8), the wild-type *SC35*-RI substrate (for Retained Intron) was poorly spliced in the presence of nuclear extract, but splicing was strongly activated upon the addition of purified recombinant SC35 (Figure 1C, lanes 2–3 and 19–20). In contrast, other SR proteins such as ASF/SF2 (lane 4) or 9G8 (8) did not activate intron excision. Interestingly, a recombinant SC35 lacking the RS domain had no activator effect and even slightly reduced splicing compared to the basal level or to the addition of RS domain-lacking ASF/SF2 (Figure 1C, lane 21 compared with 19 and 22). This dominant-negative effect of SC35ΔRS suggested that SC35 plays a direct role in splicing activation, through interactions mediated by its RS domain.

The sequence of the entire terminal intron and most of the following exon is well conserved between human and mouse *SC35* genes. In particular, a highly conserved 132 nt-long sequence, overlapping the 3′ splice site (positions −43 to +89, Figure 1B), is 100% conserved and was suggested to be involved in the control of unproductive splicing of *SC35* transcripts (12). To determine the role of this region in terminal intron splicing, we first replaced nts 7 to 73 downstream from the 3′ splice site (Figure 1B) by a neutral sequence (Supplementary Data) and analysed the splicing of this pre-mRNA *in vitro*. Both basal and SC35-activated splicing were dramatically inhibited (Figure 1C, compare lanes 5–6 to 2–3), indicating that this sequence is necessary for splicing. Mutation of the distal half of the region (44–73) also led to complete inhibition of basal splicing, but some activation was observed upon SC35 addition (lanes 13–14), indicating that this region contains an important part, but not all the elements required for intron excision. Further analysis showed that the most active elements are located within the segment 44–58 (lanes 15–16), and not in the segment 61–73 (lanes 17–18). Interestingly, substitution of the proximal half of the 70 nt sequence (7–37) inhibited the natural 3′ splice site almost completely, but weak splicing occurred at a cryptic 3′ site (position +43), due to the improvement of its polypyrimidine tract in the

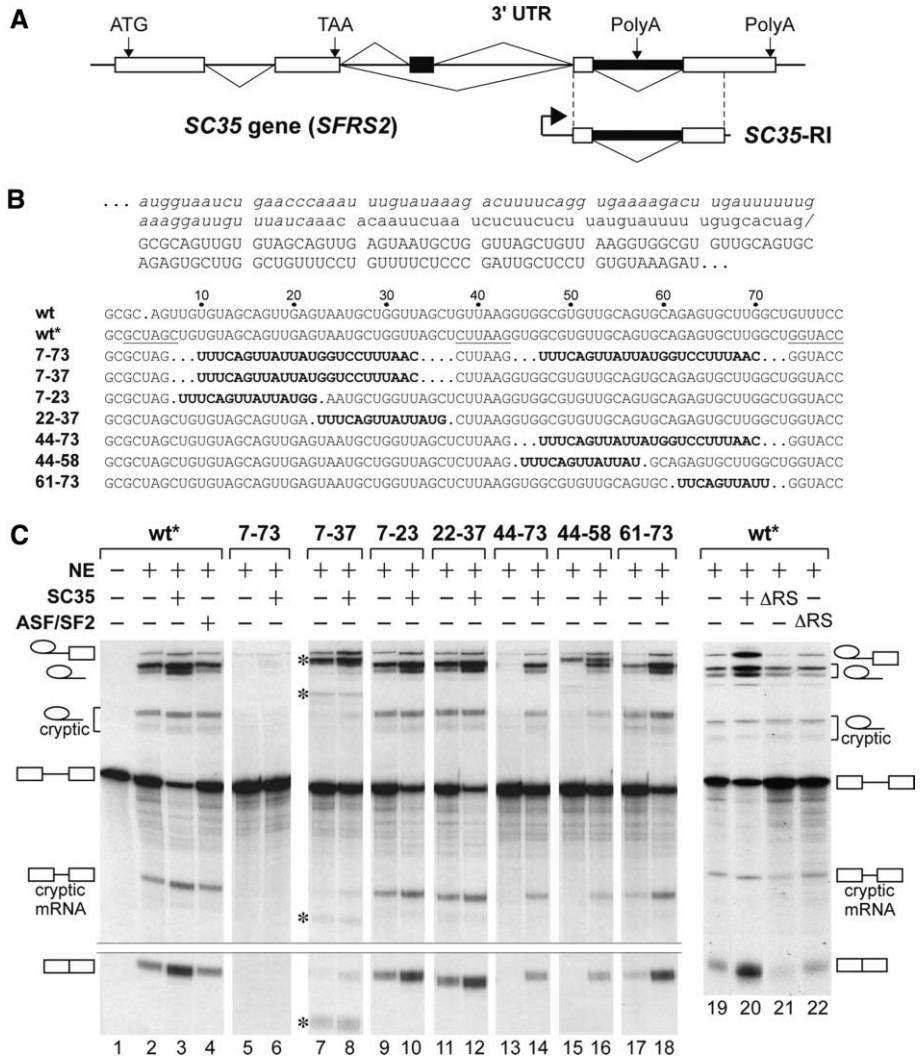

Figure 1. (**A**) Schematic organization of the *SC35* gene (*SFRS2*) and of the *SC35*-RI minigene. The open-reading frame lies within two constitutive exons, whereas the 3′ UTR is alternatively spliced and polyadenylated. The alternative cassette exon and retained intron are represented by black boxes. (**B**) Sequence of the region encompassing the 3′ splice site of terminal intron and the 5′ part of terminal exon. Intronic and exonic nucleotides are in small and capital letters, respectively. Numbers along the exonic sequence indicate the position relative to the 3′ splice site in the wild-type construct. In the wt* construct, the three newly created restriction sites are underlined. The different mutated fragments are in bold. Note that they do not systematically have the same length as the corresponding wild-type fragment. (**C**) *In vitro* splicing of wild-type and mutant *SC35*-RI transcripts. Standard splicing assays were carried out in HeLa nuclear extract, supplemented or not by 600–800 ng of purified full-length SC35, ASF/SF2 or the same proteins lacking the RS domain (ΔRS). The different pre-mRNAs are indicated above each panel. The pre-mRNA and splicing products are symbolized on the side of the gel. Products resulting from the use of an intronic cryptic 5′ splice site (intronic position +157) or from the use of an exonic cryptic 3′ splice site are indicated by the mention 'cryptic' and by an asterisk, respectively. The activity of SC35 and ASF/SF2 proteins was normalized using a control *fushi-tarazu* transcript (Supplementary Figure S1A).

mutant sequence (lanes 7–8). This cryptic site was poorly stimulated by SC35. We found also that the activatory elements were distributed all along this proximal region since the mutation of its two halves (nts 7–23 or 22–37, lanes 9–12) was without effect on splicing. All results obtained in nuclear extract were also confirmed in limiting splicing conditions, using a cytoplasmic S100 fraction complemented with purified SC35 (Supplementary Figure S1). Altogether, these results suggested the presence of several enhancer elements within the 60 nt-long region downstream from the 3′ splice site, and which contribute to SC35-mediated splicing of the upstream intron.

The terminal exon contains several SC35-dependent splicing enhancers

To confirm those results and exclude the possibility that the neutral sequence inserted in the *SC35*-RI substrate contained a strong splicing silencer, we inserted the potential ESEs into the heterologous Sp1 'inverted exon 2′ reporter (Figure 2A). Inversion of the second exon of this adenovirus E1A-derived pre-mRNA resulted in a dramatic inhibition of splicing *in vitro*, which can be restored upon insertion of an ESE (25,29). Indeed, splicing of control transcripts was nearly or completely absent, depending on the nuclear extract (Figure 2B,

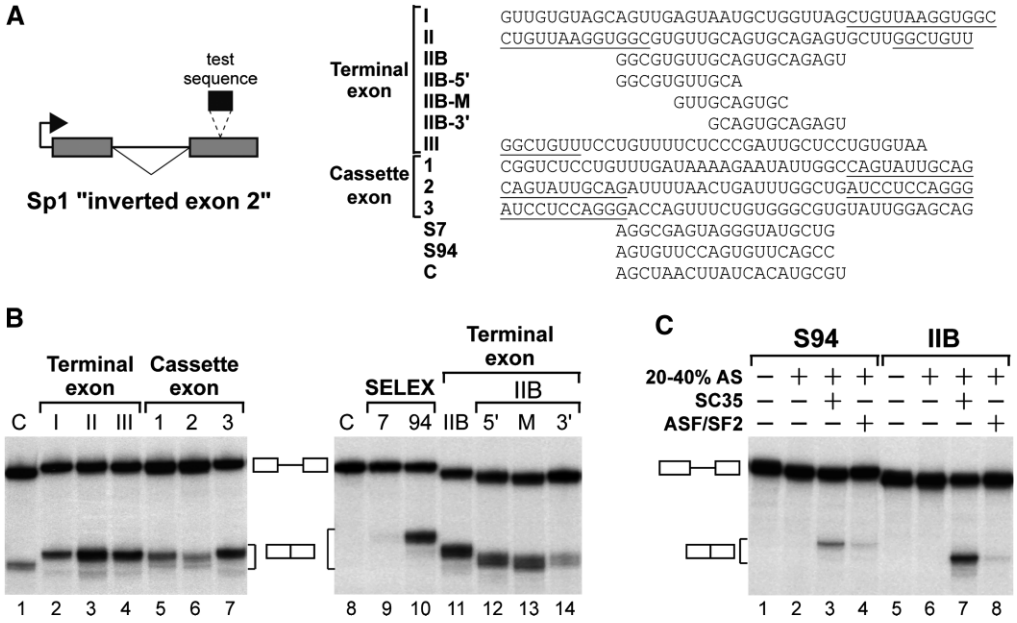

Figure 2. (**A**) Schematic view of the heterologous Sp1 'inverted exon 2' splicing substrate. Various sequences, as listed on the right side of the figure, were inserted in the middle of the inverted exon 2. Like for sequences from the terminal *SC35* exon, the fragments 1, 2 and 3 from the cassette exon partially overlap one to another (underlined nts). (**B**) Splicing assays in nuclear extract. Each transcript, harbouring one specific sequence in exon 2 as indicated, was incubated and analysed in standard conditions. (**C**) Splicing assays in cytoplasmic S100 extract. Transcripts, containing either the S-94 or the IIB sequence, were incubated in 8 µl S100 supplemented with 3 µl of a 20–40% ammonium sulphate-precipitated fraction from HeLa nuclear extract and with 400 ng of recombinant SC35 or ASF/SF2 protein. As previously shown (25,30), efficient and specific splicing activation in the S100 fraction could only be observed in the presence of this 20–40% fraction, which does not contain SR proteins.

lanes 1 and 8). In contrast, splicing activation was reproducibly observed upon insertion of each of the three tested overlapping regions of the *SC35* terminal exon [regions I (6–48), II (36–76) and III (70–106), see sequences in Figures 1B and 2A] in the inverted exon (lanes 2–4). The strongest activation was obtained with region II (Figure 2B, lane 3). Next, we progressively shortened the three regions in order to define minimal enhancer motifs. While only a weak splicing activation was observed with the subfragments of region III, indicating that no strong enhancers were present in this region (Supplementary Figure S2), the most efficient of the numerous fragments that we tested was sequence IIB (Figure 2B, lane 11, Supplementary Figure S2 and data not shown), which corresponds to the middle part of sequence II (nts 46–65, Figure 2A). Then the activation properties of three sub-fragments of sequence IIB were tested (IIB-5′, M and 3′, Figure 2A). The two overlapping segments 5′ and M, corresponding altogether to nts 46–60, exhibited strong enhancer activity (Figure 2B, lanes 12–13). Interestingly, this short ESE matched the region having the highest enhancer activity in the *SC35*-RI substrate (nts 44–58, Figure 1). In contrast, the pre-mRNA containing the IIB-3′ segment was barely spliced (Figure 2B, lane 14), in agreement with data from Figure 1.

Various RNA sequences bound by SC35 with a strong affinity have been previously identified by SELEX, however most of them, including sequences S-7 and S-94 (Figure 2A), have poor ESE activities (25,30). In addition, strong SC35-dependent ESEs may bind SC35 with a low affinity, as does the HIV-1 ESE acting at site A3 (31,32). Therefore, we wanted to determine whether splicing activation by *SC35* terminal exon ESEs is dependent on SC35 and if this is the case, what is the affinity of SC35 for these ESEs. To address the first question, we compared the SC35-dependent activation properties of these ESEs to those of SELEX sequences S-7 and S-94. As expected, sequence S-7 had no ESE activity in nuclear extract in the Sp1 reporter (Figure 2B, lane 9). In contrast, sequences IIB and S-94 had a strong ESE activity (lanes 10–11). The strong effect of sequence S-94 as compared with our previous data (25) was most likely due to different properties of the nuclear extracts used in the two studies. In fact, when assayed in an S100 fraction, which is devoid of SR proteins, the S-94-containing transcript was very weakly activated by purified SC35 (Figure 2C, lanes 1–4), showing that the splicing detected in nuclear extract was mediated by other factors. In contrast, the Sp1-IIB transcript was efficiently spliced upon addition of recombinant SC35, but not upon addition of ASF/SF2 (lanes 5–8). Splicing assays in S100 also revealed that several independent subfragments from sequences I and II have an SC35-dependent splicing activation property (data not shown). Altogether, results from Figures 1 and 2 and from Supplementary Figures S1 and S2 showed that the 5′ terminal 60 nts of the *SC35* terminal exon contain multiple SC35-dependent ESEs which are required for intron excision.

Finally, we also analysed the SC35-dependent cassette exon located within the *SC35* 3′ UTR. As for the terminal exon, we detected several SC35-dependent ESEs within

the 3′ part of the cassette exon, which corresponded to another highly conserved element (12) (Figure 2B, lanes 5–7 and data not shown). However, we did not characterize these sequences any further.

SC35 and several hnRNP proteins bind to exonic regions I and II

To address the question of SC35 binding to the different ESEs from the terminal *SC35* exon, we first performed electrophoretic mobility shift assays (EMSA). Figure 3A shows that the RNA-recognition motif (RRM) of SC35, but not that of 9G8, interacted with RNA probe IIB (lanes 1–5). However, the binding affinity was lower than with SELEX sequences S-94 and more particularly S-7 (at least six times lower) (lanes 6–9 and 11–14). Interestingly, even though those three RNA sequences present some homology (Figure 3B), their RNA-protein affinity and their ESE potential seemed to be inversely correlated: the lower the affinity of SC35 for a given sequence, the higher the ESE activity of this sequence, and vice versa.

One possible explanation could be that efficient SC35-mediated splicing requires not only binding of SC35 to an ESE, but also the binding of a cofactor. This would explain why a high affinity SC35 sequence isolated by SELEX is not sufficient *per se* to promote splicing. To identify potential SC35 coactivator(s), we performed parallel RNA affinity chromatography experiments with exonic sequences I and II that included the most proximal ESE and the ESE IIB, respectively. The experiment was carried out in splicing conditions to favour the formation of splicing-competent complexes. As negative controls, we used exonic sequence III since it was not required for terminal intron splicing (data not shown), and sequence S-7 as we postulated that coactivator(s) should not bind to this RNA. The proteins remaining bound to RNA after low-salt washes were analysed by silver staining. We observed a complex pattern of proteins and a high non-specific background (proteins bound onto the three RNAs), but bands specific for sequences I or II were detected (Supplementary Figure S3). In particular, a larger number of proteins interacted with RNA I than with other sequences. Proteins contained in the bands which were more specific to sequences I and II were identified by mass spectrometry. We found many hnRNP proteins and other RNA-binding proteins known to be involved in pre-mRNA processing or RNA stability (Supplementary Figure S3).

We then analysed the binding of some of those proteins by western blotting. This confirmed that hnRNP H, hnRNP A1 and DAZAP1 interacted only or preferentially with *SC35* sequence I (Figure 3C, compare lane 1 to other lanes). Other proteins like TDP-43 and the RNA helicase p68/DDX5 bound sequences I and II equally well and specifically (lanes 1–2). Consistent with the presence of C/U-rich stretches within sequence III, which is a good target for the splicing regulator PTB/hnRNP I, this factor was found strongly associated to this sequence and weakly to others. In contrast, PSF/SFPQ bound to each of the tested RNAs and to uncoated beads. Finally, in

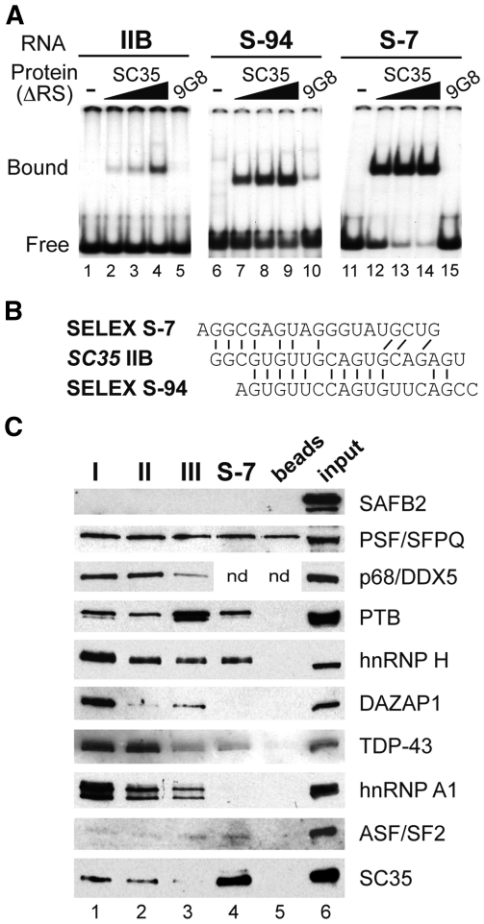

Figure 3. (**A**) Electrophoretic mobility shift assay. The complexes formed between the RNA probes (10 fmol) and GST-SC35ΔRS (10, 20 and 30 ng) or GST-9G8ΔRS (30 ng) were resolved by native gel electrophoresis to separate the protein-RNA complexes (bound) from the free RNA (free). (**B**) Sequence homology between the sequence IIB from the *SC35* terminal exon (nts 46–65) and SC35 high affinity sequences S-7 and S-94 sequences. (**C**) Western-blot of an RNA affinity experiment. Equivalent amounts of proteins retained on the different immobilized RNA probes (lanes 1 to 4), or on naked beads (lane 5) were analysed using various antibodies. The input corresponded to 1.5 µl of HeLa nuclear extract. nd: not determined.

agreement with results of Figure 3A, we observed a weak but significant binding of SC35 on sequences I and II (lanes 1–2), whereas it interacted efficiently with RNA S-7 (lane 4). The weak interaction of SC35 with sequences I and II was also confirmed by UV cross-linking of RNA-protein complexes formed in HeLa nuclear extract (Supplementary Figure S4). Other SR proteins, like ASF/SF2, or other splicing factors such as SAFB2, did not bind significantly to any of the exonic sequences (Figure 3C and data not shown). We concluded that SC35 interacts specifically with several low-affinity elements within region I/II of terminal exon, a region which is also recognized specifically (directly or indirectly) by several RNA-binding proteins.

Footprinting assays confirm the presence of several SC35 binding sites in the *SC35* terminal exon

Since the secondary structure of pre-mRNAs often plays a role in splicing regulation, we analysed the structure of the

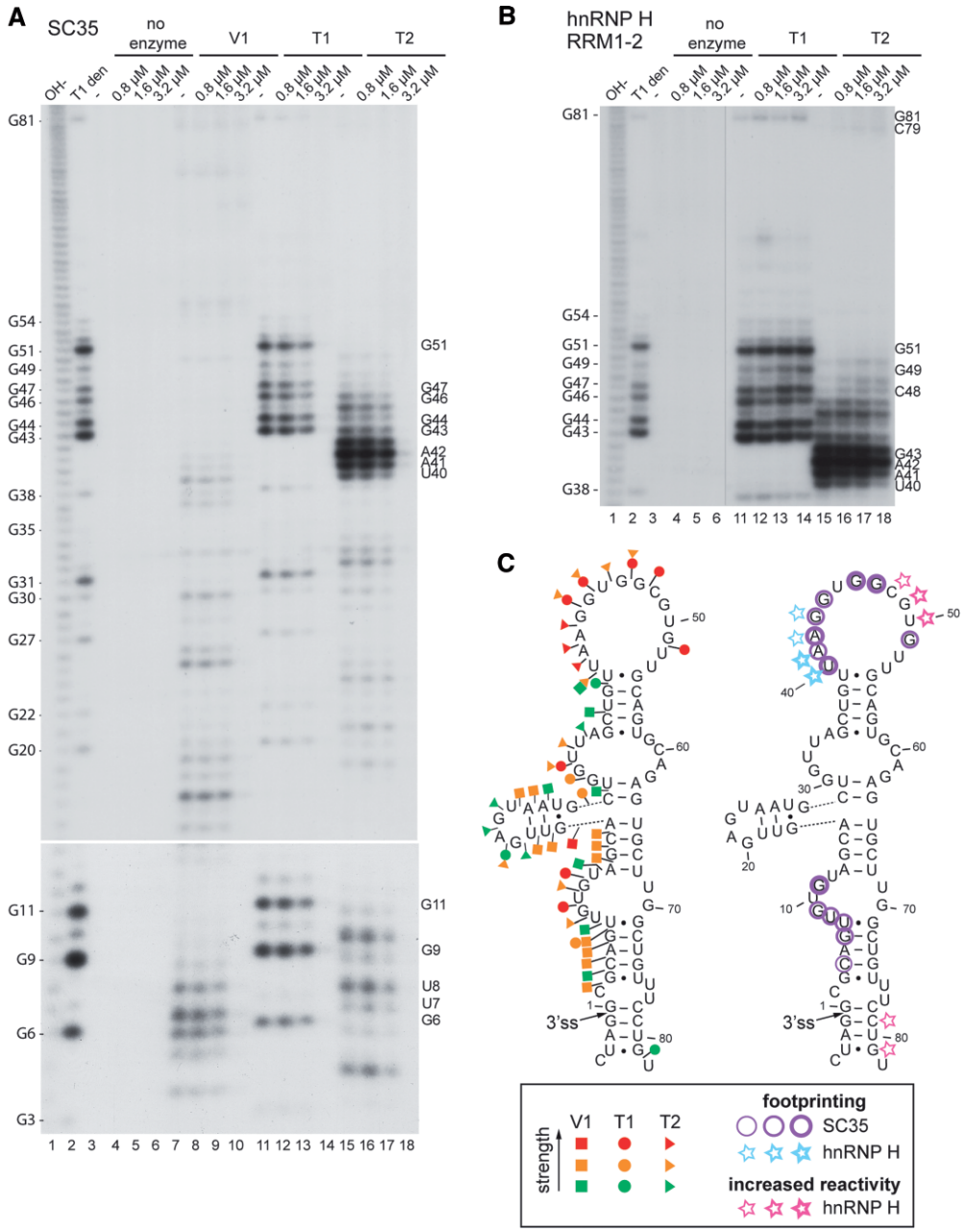

Figure 4. (**A**) The RNA was incubated in the absence (−) or in the presence of different concentrations of SC35 recombinant protein, as indicated above each lane. Digestions with RNases V1 (lanes 7–10), T1 (lanes 11–14) or T2 (lanes 15–18) were carried out as described in the 'Materials and methods' section. As a control, undigested RNA was fractionated in parallel (lanes 3–6). Lanes *OH−* and *T1 den*, corresponding respectively to alkaline hydrolysis and RNase T1 digestion in denaturing conditions, were used for localization of the cleavage sites. Nucleotides with decreased sensitivity to RNases in the presence of SC35 protein are indicated on the right. (**B**) The same experiment as in A was done using the hnRNP H RRM1-2 recombinant protein. (**C**) Secondary structure model proposed for *SC35* terminal exon. The model was proposed based on thermodynamic considerations and on the results of enzymatic digestions shown in A and B. V1, T1 and T2 RNase cleavages are represented by arrows surmounted by squares, dots and triangles, respectively. Red, orange and green symbols indicate a strong, medium or low cleavage, respectively. The residues protected by SC35 (1.6 µM) or hnRNP H RRM1-2 (3.2 µM), or having a modified sensitivity in the presence of hnRNP H RRM1-2 (3.2 µM) are circled in purple or indicated by a blue or a pink star, respectively (the line thickness is proportional to the protection strength).

enhancer/silencer region by enzymatic probing, using an RNA fragment that included the last four intronic nts and the first 106 nts of *SC35* terminal exon. Enzymatic digestion of naked RNA with RNAse V1, T1 or T2 (Figure 4A, lanes 2, 7, 11 and 15) allowed us to build a secondary structure model for the region −4 to 81, which basically consisted in a long stem-loop structure with several small internal loops (Figure 4C, left side). Interestingly, unlike the 5′ half of the stem-loop, the segment 55–80 showed no detectable sensitivity to the different enzymes, suggesting that it may be buried within the overall 3D structure.

Enzymatic footprintings were then performed using increasing concentrations of recombinant SC35 protein. At 0.8 µM SC35, we detected a weak protection of the

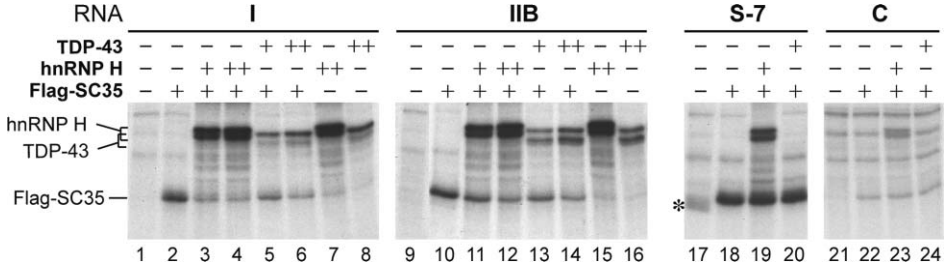

Figure 5. UV cross-linking assays. RNA probes I (lanes 1–8), IIB (lanes 9–16), S-7 (lanes 17–20) or control C (lanes 21–24) (see sequences in Figure 2A) were incubated with 2 µl of cytoplasmic extract S100 alone (lanes 1, 9, 17 and 21) or complemented with the following concentrations of purified recombinant proteins, as indicated above the figure: 400 nM FLAG-SC35, 250 and 500 nM hnRNP H, 175 and 350 nM TDP-43 (or the maximal amount of either protein added in lanes 7–8 and 15–16). Both recombinant hnRNP H and TDP-43 proteins migrated as double bands, which resulted either from premature termination of translation or from partial proteolytic digestion during the purification procedure (data not shown). The protein marked by an asterisk, which cross-linked only to the S-7 RNA in the S100 extract (lane 17), might correspond to residual amount of endogenous SC35 that escaped the nuclei during the preparation of the extract.

terminal loop and of residue G11 (Figure 4A, lanes 12 and 16 compared to lanes 11 and 15, respectively; results are summarized in Figure 4C). However, at 1.6 µM, most of the segments which were highly sensitive to RNases T1/T2 in the naked RNA (terminal loop and segment 4–11) were partially protected (lanes 13 and 17) and some of the RNase V1 cleavages disappeared (lane 9 compared with lane 7). This indicated an extended binding of SC35 to this region at this protein concentration, confirming the presence of several SC35 binding sites. When increasing the SC35 concentration to 3.2 µM, the RNA was entirely wrapped by the protein since no RNase cleavage was detected (Figure 4A, lanes 10, 14 and 18). Interestingly, initial SC35 binding seemed to occur in the apical loop, which overlaps the 5′ part of sequence IIB, and around position G24 in region I.

Splicing repressors bind exonic sequence I and II

To confirm the binding of *trans*-acting regulators to the RNA elements located within sequences I and II, we performed competition experiments using these RNAs as competitors and various *in vitro* splicing substrates (Supplementary Figure S5). As expected, these experiments highlighted the binding of splicing activator(s) to terminal exon sequences but surprisingly, they also revealed that region I, and to a lesser extent region II, are bound by at least one specific splicing repressor that specifically antagonizes the activity of the ESE IIB. Interestingly, the stronger repressor activity of sequence I correlated with the larger number of proteins interacting with this region (Figure 3 and Supplementary Figure S3).

The identification of splicing inhibitor(s) among the proteins found associated to the 5′ part of the terminal exon would have been laborious due to their elevated number. Therefore, prior to testing potential candidates, we fractionated a HeLa nuclear extract through different chromatographic steps and tested the resulting fractions for their sequence-specific repressor activity *in vitro* using the Sp1-IIB substrate (Supplementary Figure S6A and B). The most repressive fraction that we obtained was enriched in TDP-43 and hnRNP H proteins, but contained no or weak amounts of the other region I-interacting factors such as hnRNP A1, DAZAP1 or p68/DDX5 (Supplementary Figure S6C). We therefore focused our attention on those two splicing factors.

TDP-43 and hnRNP H compete with SC35 for binding to the terminal exon sequences

In order to determine whether the binding of hnRNP H and TDP-43 proteins to the enhancer/silencer region of terminal exon could interfere with SC35 binding, we carried out UV cross-linking experiments using various concentrations of recombinant proteins, in conditions (low amount of S100 extract and of competitor tRNA) which allowed a good detection of the interactions. As shown in Figure 5, recombinant SC35 protein (added to a S100 extract) cross-linked significantly to sequences I and IIB (lanes 1–2 and 9–10, respectively). Interestingly, the addition of increasing amounts of recombinant hnRNP H (lanes 3–4 and 11–12) or TDP-43 (lanes 5–6 and 13–14) proteins reduced the cross-linking of SC35 to both sequences, indicating that those two proteins directly competed with SC35 for overlapping or very nearby binding sites. This competition was probably facilitated by the weak affinity of SC35 for these regulatory sequences (Figure 3). Indeed, neither the binding of hnRNP H to sequences I and IIB, nor that of TDP-43, was significantly impaired by the addition of recombinant SC35 (compare lanes 4 and 7, 6 and 8, 12 and 15, 14 and 16). In fact, only a 3-times higher SC35 concentration could slightly reduce hnRNP H binding, but not TDP-43 binding (data not shown). Finally, although hnRNP H (but not TDP-43) also cross-linked with sequence S-7, it could not inhibit the strong interaction between SC35 and this sequence (lanes 17–20), either because the affinity of SC35 for this sequence is too strong, or because the binding sites of both proteins do not overlap. A similar result was observed with an unrelated control sequence, although the interactions of SC35 and hnRNP H with this sequence were very weak (lanes 21–24).

We next carried out footprinting assays with the hnRNP H N-terminal RRMs 1 and 2, responsible for specific RNA recognition (33) to identify the binding sites for this protein. The results of these experiments (Figures 4B and 4C) revealed an increased reactivity

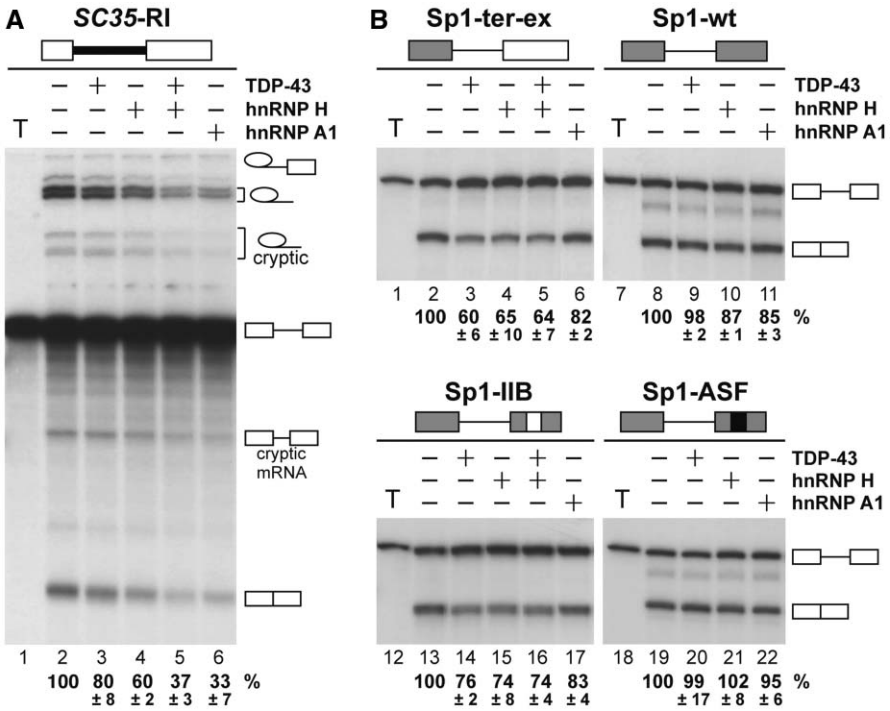

Figure 6. (**A**) Repression of *SC35*-RI pre-mRNA splicing by hnRNP proteins. The transcript is schematized on top of the figure. Splicing was carried out in standard conditions in the absence or presence of 300, 320 or 480 ng of purified recombinant GST-hnRNP H, hnRNP A1 or GST-TDP-43, respectively, or half of those amounts when two proteins were added together. Splicing efficiencies were calculated as in Supplementary Figure S5 and are indicated under each lane. (**B**) Splicing of Sp1-derived pre-mRNA in the presence of recombinant hnRNP proteins. The different transcripts are schematized on top of each panel. The common backbone derived from the wild-type Sp1 pre-mRNA (top right panel) is represented by grey boxes. The white box in the chimeric Sp1-ter-ex transcript symbolizes the terminal exon from the *SC35*-RI transcript, while the minimal *SC35* IIB sequence and the control ASF/SF2-specific sequence are represented by a small white (Sp1-IIB) or black (Sp1-ASF) box, respectively. The experiment was carried out as in A.

in the 3′ part of the terminal loop (segment 48–50), which overlaps sequence IIB, and a weak increase of the reactivity of residues 79 and 81. Such variations suggest that hnRNP H induced a modification of the RNA structure, in contrast to what we observed with SC35. Most importantly, however, we observed also a strong protection of the segment 40–45, which overlaps regions I and II and corresponds to one of the major SC35 binding sites (Figure 4A and C).

Altogether, results of Figures 4 and 5 indicated that hnRNP H and TDP-43, two proteins which are enriched in a fraction that represses SC35-mediated splicing, have binding sites which overlap those of SC35 within the terminal exon, and that both proteins efficiently and specifically compete the low-affinity binding of SC35 to that region.

TDP-43 and hnRNP H inhibit splicing of *SC35* terminal intron *in vitro*

We next addressed directly the potential repressive effect of hnRNP H and TDP-43 on *SC35* terminal intron splicing, using *in vitro* splicing assays. As shown in Figure 6A, recombinant TDP-43 and hnRNP H proteins both inhibited moderately the splicing of the *SC35*-RI transcript (lanes 3 and 4 compared to lane 2), but they had a cooperative effect when added together (lane 5), inhibiting splicing by over 60%. Despite its complete absence in our enriched repressor fraction (Supplementary Figure S6C), hnRNP A1 also inhibited strongly the splicing of this pre-mRNA (lane 6). However, this effect was not dependent on the presence of the terminal *SC35* exon since hnRNP A1 inhibited weakly and equally the chimeric Sp1-ter-ex and the control Sp1-wt transcripts (Figure 6B, lanes 6 and 11 compared with lanes 2 and 8). In contrast, TDP-43 and hnRNP H inhibited specifically Sp1-ter-ex splicing (40 and 35% inhibition, respectively) (lanes 3–4 and 9–10). Similarly, the Sp1 transcript containing the sequence IIB, but not an ASF/SF2-specific sequence, was also inhibited by TDP43 and hnRNP H (Figure 6B, lanes 13–16 and lanes 19–21), while only a weak inhibition was observed with hnRNP A1 (lanes 17 and 22). We concluded that TDP-43 and hnRNP H inhibit terminal *SC35* intron splicing *in vitro* in a sequence-specific manner.

In this last experiment using the Sp1-IIB transcript, the level of inhibition by TDP-43 and hnRNP H (about 25%) was lower than with the Sp1-ter-ex transcript, most likely because less potential binding sites were available, in agreement with the results of footprinting experiments using the RNA-binding domains of hnRNP H (Figure 4). Finally, it is also interesting to note that unlike for *SC35*-RI transcripts, we did not observe any cooperative effect of TDP-43 and hnRNP H with Sp1-derived substrates (Figure 6B, lanes 3–5 and 14–16), suggesting that

inhibition of terminal intron splicing is more complex in the original sequence environment and may involve other binding sites within the regulated intron or in the upstream exon.

TDP-43 and hnRNP H repress the terminal *SC35* 3′ splice site *in cellulo*

To confirm our results in a cellular context, we designed a minigene that recapitulated SC35-dependent activation of terminal *SC35* 3′ splice site. We introduced a fragment of the *SC35* gene, spanning the 3′ part of terminal intron and the regulatory exonic region, into the β-globin intron of a CMV promoter-driven plasmid. The resulting minigene (p*SC35*-βGlo, Figure 7A) had two alternative 3′ splice sites and its splicing in HeLa cells, as analysed by RT-PCR, resulted in the formation of two main products, corresponding to mRNAs spliced at the β-globin (lower band) or *SC35* (upper band) 3′ splice site (Figure 7B, lane 1). As expected, co-transfection of GFP-tagged SC35 stimulated the use of the *SC35* 3′ splice site by over 3-fold (lane 2). A similar result was obtained when endogenous SC35 expression was increased upon treatment of cells with caffeine (34) (Figure 7B, lanes 9–10, Figure 7C). In contrast, targeting the *SC35* gene with small-interfering RNAs (siRNA), even though the global level of SC35 protein was reduced only by about a half, resulted in a strong inhibition of the *SC35* 3′ splice site (Supplementary Figure S7). These results indicated that our substrate responded specifically to changes in endogenous SC35 levels.

We next tested the effect of hnRNP H or TDP-43 on the minigene. Unlike what we observed *in vitro*, over-expression of hnRNP H did not repress the use of the *SC35* 3′ splice site, and even had a moderate opposite effect (Figure 7B, lane 3). However, silencing of hnRNP H expression led to an increase in '*SC35*' mRNA relative to β-globin mRNA (Figure 7E and 7D, compare lanes 1 and 3), indicating that hnRNP H has a direct or an indirect negative effect on the *SC35* 3′ splice site. We obtained the same result with two different siRNAs, targeting both hnRNP H and F, confirming that splicing modulation was due to the specific depletion of these two proteins. Similarly, over-expression and depletion of TDP-43 did not provide fully consistent results: nearly complete silencing of TDP-43 gene using two distinct siRNA (Figure 7E and data not shown) had no significant effect on splicing (Figure 7D, lane 4). Yet, over-expression of TDP-43 led to a dramatic inhibition of the *SC35* 3′ splice site (Figure 7B, lane 4). Interestingly, TDP-43 overcame the GFP-SC35-mediated activation of splicing

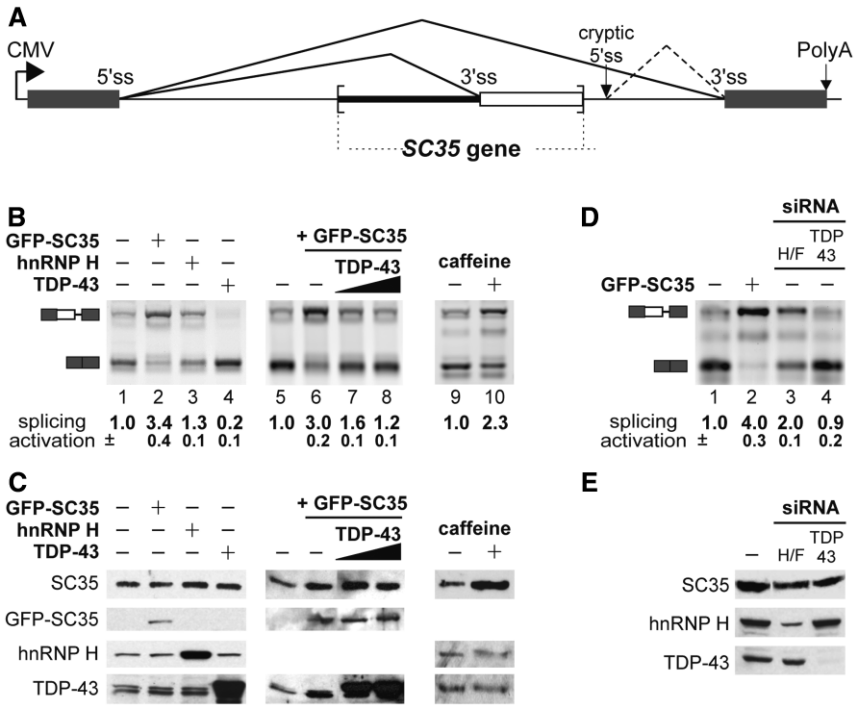

Figure 7. (**A**) Schematic structure of the p*SC35*-βGlo minigene. A fragment of the *SC35* gene including the 3′ part of the retained terminal intron (thick black line) and the 5′ part of the terminal exon (white box) was inserted in the rabbit β-globin intron 2, creating a reporter with alternative 3′ splice sites (splicing is represented by broken filled lines). When the *SC35* 3′ splice site was used, a cryptic 5′ splice site located downstream from the insert, within the 3′ part of the β-globin intron, was systematically activated (broken dotted line), creating an 'SC35' alternative exon. (**B**) and (**C**) RNA and protein analysis after transfection of HeLa cells. Cells were cotransfected with the p*SC35*-βGlo minigene and plasmids carrying various cDNAs as indicated above the gels. RNA and protein samples were extracted and analysed respectively by RT-PCR (B) or western blotting (C) with specific antibodies, as indicated. Anti-GFP was used to monitor the amount of GFP-SC35 protein, which could not be detected using anti-SC35 antibodies due to its low level of expression. AS gave rise to two major mRNA products depending on the use of the β-globin (lower band) or *SC35* (upper band) 3′ splice site. (**D**) and (**E**) RNA and protein analysis after siRNA-mediated knockdown of hnRNP H/F or TDP-43. RT-PCR analysis and quantification of mRNA products (D) was as in panel B. Efficiency of silencing and endogenous level of SC35 protein were monitored by western-blotting (E) as in panel C.

in a concentration-dependent manner (Figure 7B, lanes 7–8 compared to lane 6, and Figure 7C), indicating a competition between the two proteins for regulating the *SC35* 3′ splice site. No further inhibition was observed when we co-expressed TDP-43 and hnRNP H (data not shown). Importantly, the level of endogenous SC35 remained constant in all experiments (Figure 7C and E), indicating that the effects were primarily due to the over-expression/depletion of the corresponding proteins, although we could not exclude the contribution of uncharacterized secondary effects. Altogether, our results confirmed our *in vitro* data and showed that hnRNP H and TDP-43 both repress the *SC35* 3′ splice site *in cellulo* in a manner antagonistic to SC35.

DISCUSSION

Splicing activation by SC35

In a previous report, we showed that SC35 regulates its own expression by promoting specific AS reactions within the 3′ UTR of its pre-mRNA, resulting mostly in the formation of 1.6 and 1.7 kb mRNA isoforms in which the terminal intron has been spliced out (8). The instability of these isoforms is due to the activation of NMD (8,11–13), confirming the existence of a negative feedback loop for SC35. In the present study, we identified a 60-nt sequence within the terminal *SC35* exon, which is required for SC35-mediated splicing of the retained intron. The most active elements are located within overlapping segments IIB-5′ and IIB-M of the 20-nt sequence IIB (Figure 2 and Supplementary Figure S2). Systematic mutagenesis of this sequence suggested that the core motif GUUGCAGU is essential for ESE activity, but that flanking sequences are also important (Supplementary Figure S2). We also found some highly conserved regulatory elements within the 3′ part of the *SC35* cassette exon, which present some homology with the ESE IIB (data not shown). A comparison of the IIB element to other SC35-specific ESEs (Supplementary Table S1) showed a large variety of motifs, and no unique consensus sequence could be defined. Some motifs found in the ESE IIB, the SELEX S-94 sequence (see an alignment of these 2 sequences in Figure 3B) and the β-globin gene (35) are similarly rich in pyrimidines. In contrast, other ESEs are more purine-rich (Supplementary Table S1), whereas a C-rich consensus sequence was identified by functional selection of SC35-responsive ESEs (36). As the ESEfinder program was based on this last consensus sequence (37), it only predicted low-score SC35 motifs within the 60-nt ESE of *SC35* terminal exon (Supplementary Figure S8).

Unlike high-affinity SC35 SELEX sequences which have poor ESE activity, the potent ESE IIB and other SC35-binding sites within the 60-nt ESE were recognized only weakly by the SC35 RRM or by endogenous SC35 within a nuclear extract (Figure 3). Several hypotheses can be raised to explain this discrepancy. It is possible that a strong interaction between the SC35 RRM and RNA does not confer enough mobility to the protein to develop other interactions that are necessary for splicing activation. Alternatively, efficient activation by SC35 might require the binding of a cofactor(s) near low-affinity SC35 binding sites. This may be required to assemble an active SC35 enhancer complex, similarly to the assembly of enhancer complexes to *Drosophila doublesex* purine-rich elements (38). Sequences selected by SELEX using purified SC35 would not contain the cofactor binding site and would therefore be inactive in splicing assays. The factors which we found to bind specifically to the SC35-responsive ESE are potential cofactors. However, the over-expression or knockdown of several candidates (such as DAZAP1 and p68/DDX5) did not affect SC35-dependent use of terminal 3′ splice site *in cellulo* (data not shown).

Interestingly, our footprinting experiments indicated that the most active SC35-responsive motif (IIB) overlaps with the most accessible SC35-binding site in a 14-nt single-stranded loop that caps a long stem-loop region (Figure 4). However, in agreement with results from Figure 3, which suggested the existence of several SC35 binding sites in the regulatory region, it became entirely protected from enzymatic degradation at higher SC35 concentration (Figure 4). It is possible that the apical loop represents a primary binding site for the protein, which would promote the binding of SC35 molecules to other sites along the 60-nt region. Similar mechanisms have been described for hnRNP A1 or SC35 binding on HIV-1 transcripts (31,32). Our footprinting experiments suggest that hnRNP H may modify the RNA structure upon binding and might alter the binding and/or the effect of other splicing regulators. The fact that p68 binds to the regulatory region also raised the hypothesis that this RNA helicase may have a similar effect. Remodeling of an RNA structure by p68 was recently proposed to regulate the inclusion of H-Ras exon IDX by decreasing the binding of hnRNP H (39). However, our experiments did not support a direct effect of p68 on the splicing of the p*SC35*-βGlo minigene *in cellulo* (data not shown).

Repression by TDP-43 and hnRNP H

About a dozen of RNA-binding proteins bound specifically to the regulatory region downstream from the retained *SC35* intron. At least two of them, TDP-43 and hnRNP H, but not hnRNP A1, repressed splicing in a sequence-specific manner *in vitro* and *in cellulo*. Both TDP-43 and hnRNP H, which respectively recognize UG repeats and GGG-containing motifs, are well-known AS regulators (4,40). We could not carry out footprinting analysis using the full-length recombinant proteins, due to their poor solubility. Interestingly however, the 60-nt regulatory region of the *SC35* terminal exon contains a few potential TDP-43 binding sites, whereas it does not contain any G triplet. In fact, the major binding site for the hnRNP H RNA binding domains is a UAAGG motif located in the apical stem-loop, which overlaps an SC35-binding site and which likely explains the direct competition that we observed between the two antagonistic factors (Figure 5). However, only TDP-43, but not hnRNP H, competed the effect of SC35 and repressed

the *SC35* 3′ splice site *in cellulo* in a concentration-dependent manner (Figure 7). The absence of effect of over-expressed hnRNP H could be due to the high endogenous level of hnRNP H in HeLa cells, which is consistent with the basal repressed state of this 3′ splice site and with its stimulation upon hnRNP H knock-down. HnRNP F, which was also targeted in our siRNA experiments, may also be a repressor of the 3′ splice site, since this protein has similar functions to hnRNP H. However, it is unlikely to be the main repressor for two reasons: hnRNP H efficiently inhibited splicing *in vitro* in a sequence-specific manner (Figure 6), and hnRNP F was not enriched in the repressor fraction that inhibited splicing of the Sp1-IIB substrate *in vitro* (Supplementary Figure S6C).

TDP-43 specifically repressed splicing of *SC35* 3′ splice site both *in vitro* and *in cellulo*, but its knock-down did not have any effect on splicing. The most likely explanation is that the repression could result from a combined action of several factors: hnRNP H could play a key role in triggering splicing inhibition by competing directly the binding of SC35, while TDP-43 may only promote further repression when its expression is increased, possibly by preventing the expansion of SC35 binding along the enhancer region. It is also possible that other proteins among those that we identified are involved in splicing repression *in vivo*. The AU-rich binding proteins AUF1/hnRNP D and KSRP/FBP2 are frequently found associated to 3′ UTRs and might be involved in other aspects of mRNA metabolism such as stability or transport. However, several of the factors identified can modulate AS (4,41), and efficient inhibition could result from the assembly of a multi-protein complex containing a combination of those factors.

Consequences for the regulation of SC35 expression *in vivo*

Our cross-linking and titration experiments (Figure 5 and Supplementary Figure S4) indicate that repressors have a stronger affinity than SC35 for the regulatory region. This suggests that SC35 could activate splicing only when a threshold concentration is reached to overcome the binding of repressors and to occupy most binding sites along the 60-nt region. This model is functionally sound since it would provide a finely tuned negative control of SC35 expression: splicing of terminal intron and NMD-mediated degradation of mRNAs would only occur when SC35 concentration becomes too elevated. Although the proper regulation of AS in cells likely tolerates some variations in the concentration of SC35, such a safeguard mechanism might be essential since SC35 plays important roles in the control of cell proliferation (9,10).

In fact, the treatment of cultured HeLa or nasal epithelial cells with NMD inhibitors revealed the presence of significant amounts of *SC35* 1.6/1.7 kb mRNA isoforms, which result from splicing activation by SC35 (8,11–13). This indicates that terminal intron can be spliced out in standard cell growing conditions. Similarly, transfection of HeLa cells with our minigene also showed a significant basal use of terminal *SC35* 3′ splice site (Figure 7). A prediction from those results is that SC35 concentration should not increase strongly when *SC35* gene transcription is increased. Yet, a 3–4-fold increase of SC35 concentration has been reported in several well-defined biological conditions, in apparent contradiction with the concept of feedback regulatory loop. For example, caffeine treatment of various cells, including HeLa cells, induced an increase of SC35 protein level (34) (Figure 7), through a mechanism which is not well understood. However, the same caffeine concentration can also inhibit NMD (42), so it cannot be ruled out that the 1.6/1.7 kb mRNA isoforms were stabilized, increasing the overall concentration of SC35 mRNA and protein.

Another recent study showed that over-expression of the transcription factor E2F1 directly stimulated the transcription of the *SC35* gene and the synthesis of SC35 protein in human lung carcinoma cells (43). The basal SC35 concentration seemed weaker in this cell line than in mouse embryonic fibroblasts, suggesting that SC35 was present in suboptimal amounts and that its increased concentration was tolerated as being below the critical threshold level that triggers the feedback loop. Moreover, E2F1 stimulates cell cycle progression, and a recent study reported that proliferating cells tend to express mRNAs with shorter 3′ UTR regions compared to nonactivated cells (44). E2F1 may induce the synthesis of specific *SC35* transcripts using the proximal poly-A site, which is located in the terminal intron (Figure 1), leading to the accumulation of the 1.3 kb, NMD-insensitive mRNA isoform and to an increase in SC35 protein synthesis.

The presence of important splicing regulatory elements in the 3′ UTR of the *SC35* gene, that we demonstrated for the first time in this study, gives one explanation for the extreme conservation of this region in vertebrates (the regulatory 60-nt region is nearly 100% conserved from human to xenopus). Even though this extreme conservation could also reflect, for example, the presence of binding sites for microRNAs or for factors regulating the stability of the mRNAs, our findings support the hypothesis that was raised following the identification of similar highly conserved or ultraconserved elements associated to AS-NMD events in the pre-mRNAs of many splicing factors (12,21,23). One can anticipate that the expression of a large proportion of splicing regulators is controlled in similar ways as that of SC35, through an intricate interplay of self- and cross-regulatory mechanisms. This may provide the cells with a way to maintain the homeostasis of those factors to ensure that splicing does not escape control. It also offers multiple ways of modifying transiently the relative expression of specific factors, which is one of the keys for controlling AS choices.

SUPPLEMENTARY DATA

Supplementary Data are available at NAR Online.

ACKNOWLEDGEMENTS

The authors are grateful to Manuela Argentini for her help with mass spectrometry analysis. They thank

D. Auboeuf, D. Black, E. Buratti, G. Dreyfuss, D. Elliott, S. Rousseau and J. Soret for the generous gift of antibodies and plasmids.

FUNDING

Institut National de la Santé et de la Recherche Médicale, the Centre National de la Recherche Scientifique and the Universities of Strasbourg and Nancy, and grants from the Agence Nationale pour la Recherche (ANR-05-BLAN-0261-01 to J.S. and Ch.B.); European Commission (EURASNET NoE to J.S. and Ch.B.). Funding for open access charge: IGBMC.

Conflict of interest statement. None declared.

REFERENCES

1. Wang,Z. and Burge,C.B. (2008) Splicing regulation: from a parts list of regulatory elements to an integrated splicing code. *RNA*, **14**, 802–813.
2. Bourgeois,C.F., Lejeune,F. and Stevenin,J. (2004) Broad specificity of SR (serine/arginine) proteins in the regulation of alternative splicing of pre-messenger RNA. *Prog. Nucleic Acid Res. Mol. Biol.*, **78**, 37–88.
3. Long,J.C. and Caceres,J.F. (2009) The SR protein family of splicing factors: master regulators of gene expression. *Biochem. J.*, **417**, 15–27.
4. Martinez-Contreras,R., Cloutier,P., Shkreta,L., Fisette,J.F., Revil,T. and Chabot,B. (2007) hnRNP proteins and splicing control. *Adv. Exp. Med. Biol.*, **623**, 123–147.
5. Pandit,S., Wang,D. and Fu,X.D. (2008) Functional integration of transcriptional and RNA processing machineries. *Curr. Opin. Cell Biol.*, **20**, 260–265.
6. Buratti,E. and Baralle,F.E. (2004) Influence of RNA secondary structure on the pre-mRNA splicing process. *Mol. Cell. Biol.*, **24**, 10505–10514.
7. McGlincy,N.J. and Smith,C.W. (2008) Alternative splicing resulting in nonsense-mediated mRNA decay: what is the meaning of nonsense? *Trends Biochem. Sci.*, **33**, 385–393.
8. Sureau,A., Gattoni,R., Dooghe,Y., Stevenin,J. and Soret,J. (2001) SC35 autoregulates its expression by promoting splicing events that destabilize its mRNAs. *EMBO J.*, **20**, 1785–1796.
9. Wang,H.Y., Xu,X., Ding,J.H., Bermingham,J.R. Jr and Fu,X.D. (2001) SC35 plays a role in T cell development and alternative splicing of CD45. *Mol. Cell*, **7**, 331–342.
10. Xiao,R., Sun,Y., Ding,J.H., Lin,S., Rose,D.W., Rosenfeld,M.G., Fu,X.D. and Li,X. (2007) Splicing regulator SC35 is essential for genomic stability and cell proliferation during mammalian organogenesis. *Mol. Cell. Biol.*, **27**, 5393–5402.
11. Gehring,N.H., Kunz,J.B., Neu-Yilik,G., Breit,S., Viegas,M.H., Hentze,M.W. and Kulozik,A.E. (2005) Exon-junction complex components specify distinct routes of nonsense-mediated mRNA decay with differential cofactor requirements. *Mol. Cell*, **20**, 65–75.
12. Lareau,L.F., Inada,M., Green,R.E., Wengrod,J.C. and Brenner,S.E. (2007) Unproductive splicing of SR genes associated with highly conserved and ultraconserved DNA elements. *Nature*, **446**, 926–929.
13. Linde,L., Boelz,S., Nissim-Rafinia,M., Oren,Y.S., Wilschanski,M., Yaacov,Y., Virgilis,D., Neu-Yilik,G., Kulozik,A.E., Kerem,E. *et al.* (2007) Nonsense-mediated mRNA decay affects nonsense transcript levels and governs response of cystic fibrosis patients to gentamicin. *J. Clin. Invest.*, **117**, 683–692.
14. Jumaa,H. and Nielsen,P.J. (1997) The splicing factor SRp20 modifies splicing of its own mRNA and ASF/SF2 antagonizes this regulation. *EMBO J.*, **16**, 5077–5085.
15. Lejeune,F., Cavaloc,Y. and Stevenin,J. (2001) Alternative splicing of intron 3 of the serine/arginine-rich protein 9G8 gene. Identification of flanking exonic splicing enhancers and involvement of 9G8 as a trans-acting factor. *J. Biol. Chem.*, **276**, 7850–7858.
16. Stoilov,P., Daoud,R., Nayler,O. and Stamm,S. (2004) Human tra2-beta1 autoregulates its protein concentration by influencing alternative splicing of its pre-mRNA. *Hum. Mol. Genet.*, **13**, 509–524.
17. Le Guiner,C., Lejeune,F., Galiana,D., Kister,L., Breathnach,R., Stevenin,J. and Del Gatto-Konczak,F. (2001) TIA-1 and TIAR activate splicing of alternative exons with weak 5′ splice sites followed by a U-rich stretch on their own pre-mRNAs. *J. Biol. Chem.*, **276**, 40638–40646.
18. Boutz,P.L., Stoilov,P., Li,Q., Lin,C.H., Chawla,G., Ostrow,K., Shiue,L., Ares,M. Jr and Black,D.L. (2007) A post-transcriptional regulatory switch in polypyrimidine tract-binding proteins reprograms alternative splicing in developing neurons. *Genes Dev.*, **21**, 1636–1652.
19. Spellman,R., Llorian,M. and Smith,C.W. (2007) Crossregulation and functional redundancy between the splicing regulator PTB and its paralogs nPTB and ROD1. *Mol. Cell*, **27**, 420–434.
20. Barberan-Soler,S. and Zahler,A.M. (2008) Alternative splicing regulation during C. elegans development: splicing factors as regulated targets. *PLoS Genet.*, **4**, e1000001.
21. Ni,J.Z., Grate,L., Donohue,J.P., Preston,C., Nobida,N., O'Brien,G., Shiue,L., Clark,T.A., Blume,J.E. and Ares,M. Jr (2007) Ultraconserved elements are associated with homeostatic control of splicing regulators by alternative splicing and nonsense-mediated decay. *Genes Dev.*, **21**, 708–718.
22. Saltzman,A.L., Kim,Y.K., Pan,Q., Fagnani,M.M., Maquat,L.E. and Blencowe,B.J. (2008) Regulation of multiple core spliceosomal proteins by alternative splicing-coupled nonsense-mediated mRNA decay. *Mol. Cell. Biol.*, **28**, 4320–4330.
23. Bejerano,G., Pheasant,M., Makunin,I., Stephen,S., Kent,W.J., Mattick,J.S. and Haussler,D. (2004) Ultraconserved elements in the human genome. *Science*, **304**, 1321–1325.
24. Venables,J.P., Bourgeois,C.F., Dalgliesh,C., Kister,L., Stevenin,J. and Elliott,D.J. (2005) Up-regulation of the ubiquitous alternative splicing factor Tra2beta causes inclusion of a germ cell-specific exon. *Hum. Mol. Genet.*, **14**, 2289–2303.
25. Cavaloc,Y., Bourgeois,C.F., Kister,L. and Stevenin,J. (1999) The splicing factors 9G8 and SRp20 transactivate splicing through different and specific enhancers. *RNA*, **5**, 468–483.
26. Gallego,M.E., Gattoni,R., Stevenin,J., Marie,J. and Expert-Bezancon,A. (1997) The SR splicing factors ASF/SF2 and SC35 have antagonistic effects on intronic enhancer-dependent splicing of the beta-tropomyosin alternative exon 6A. *EMBO J.*, **16**, 1772–1784.
27. Jacquenet,S., Ropers,D., Bilodeau,P.S., Damier,L., Mougin,A., Stoltzfus,C.M. and Branlant,C. (2001) Conserved stem-loop structures in the HIV-1 RNA region containing the A3 3′ splice site and its cis-regulatory element: possible involvement in RNA splicing. *Nucleic Acids Res.*, **29**, 464–478.
28. Mathews,D.H., Sabina,J., Zuker,M. and Turner,D.H. (1999) Expanded sequence dependence of thermodynamic parameters improves prediction of RNA secondary structure. *J. Mol. Biol.*, **288**, 911–940.
29. Disset,A., Bourgeois,C.F., Benmalek,N., Claustres,M., Stevenin,J. and Tuffery-Giraud,S. (2006) An exon skipping-associated nonsense mutation in the dystrophin gene uncovers a complex interplay between multiple antagonistic splicing elements. *Hum. Mol. Genet.*, **15**, 999–1013.
30. Tacke,R. and Manley,J.L. (1995) The human splicing factors ASF/SF2 and SC35 possess distinct, functionally significant RNA binding specificities. *EMBO J.*, **14**, 3540–3551.
31. Zhu,J., Mayeda,A. and Krainer,A.R. (2001) Exon identity established through differential antagonism between exonic splicing silencer-bound hnRNP A1 and enhancer-bound SR proteins. *Mol. Cell*, **8**, 1351–1361.
32. Hallay,H., Locker,N., Ayadi,L., Ropers,D., Guittet,E. and Branlant,C. (2006) Biochemical and NMR study on the competition between proteins SC35, SRp40, and heterogeneous nuclear ribonucleoprotein A1 at the HIV-1 Tat exon 2 splicing site. *J. Biol. Chem.*, **281**, 37159–37174.
33. Dominguez,C. and Allain,F.H. (2006) NMR structure of the three quasi RNA recognition motifs (qRRMs) of human hnRNP F and interaction studies with Bcl-x G-tract RNA: a novel mode of RNA recognition. *Nucleic Acids Res.*, **34**, 3634–3645.

34. Shi,J., Hu,Z., Pabon,K. and Scotto,K.W. (2008) Caffeine regulates alternative splicing in a subset of cancer-associated genes: a role for SC35. *Mol. Cell. Biol.*, **28**, 883–895.
35. Schaal,T.D. and Maniatis,T. (1999) Multiple distinct splicing enhancers in the protein-coding sequences of a constitutively spliced pre-mRNA. *Mol. Cell. Biol.*, **19**, 261–273.
36. Liu,H.X., Chew,S.L., Cartegni,L., Zhang,M.Q. and Krainer,A.R. (2000) Exonic splicing enhancer motif recognized by human SC35 under splicing conditions. *Mol. Cell. Biol.*, **20**, 1063–1071.
37. Cartegni,L., Wang,J., Zhu,Z., Zhang,M.Q. and Krainer,A.R. (2003) ESEfinder: a web resource to identify exonic splicing enhancers. *Nucleic Acids Res.*, **31**, 3568–3571.
38. Lynch,K.W. and Maniatis,T. (1996) Assembly of specific SR protein complexes on distinct regulatory elements of the Drosophila doublesex splicing enhancer. *Genes Dev.*, **10**, 2089–2101.
39. Camats,M., Guil,S., Kokolo,M. and Bach-Elias,M. (2008) P68 RNA helicase (DDX5) alters activity of cis- and trans-acting factors of the alternative splicing of H-Ras. *PLoS ONE*, **3**, e2926.
40. Buratti,E. and Baralle,F.E. (2008) Multiple roles of TDP-43 in gene expression, splicing regulation, and human disease. *Front. Biosci.*, **13**, 867–878.
41. Goina,E., Skoko,N. and Pagani,F. (2008) Binding of DAZAP1 and hnRNPA1/A2 to an exonic splicing silencer in a natural BRCA1 exon 18 mutant. *Mol. Cell. Biol.*, **28**, 3850–3860.
42. Usuki,F., Yamashita,A., Higuchi,I., Ohnishi,T., Shiraishi,T., Osame,M. and Ohno,S. (2004) Inhibition of nonsense-mediated mRNA decay rescues the phenotype in Ullrich's disease. *Ann. Neurol.*, **55**, 740–744.
43. Merdzhanova,G., Edmond,V., De Seranno,S., Van den Broeck,A., Corcos,L., Brambilla,C., Brambilla,E., Gazzeri,S. and Eymin,B. (2008) E2F1 controls alternative splicing pattern of genes involved in apoptosis through upregulation of the splicing factor SC35. *Cell Death Differ.*, **15**, 1815–1823.
44. Sandberg,R., Neilson,J.R., Sarma,A., Sharp,P.A. and Burge,C.B. (2008) Proliferating cells express mRNAs with shortened 3′ untranslated regions and fewer microRNA target sites. *Science*, **320**, 1643–1647.